Paper:

Development of Building Height Data in Peru from High-Resolution SAR Imagery

Wen Liu[*], **Fumio Yamazaki**[*], **Bruno Adriano**[**], **Erick Mas**[***],
and Shunichi Koshimura[***]

[*]Graduate School of Engineering, Chiba University
1-33 Yayoi-cho, Inageku, Chiba 263-8522, Japan
E-mail: wen.liu@chiba-u.jp
[**]Graduate School of Engineering, Tohoku University, Sendai, Japan
[***]International Research Institute of Disaster Science (IRIDeS),
Tohoku University, Sendai, Japan

[Received July 30, 2014; accepted September 17, 2014]

Building data, such as footprint and height, are important information for pre- and post-event damage assessments when natural disasters occur. However, these data are not easily available in many countries. Because of the remarkable improvements in radar sensors, high-resolution (HR) Synthetic Aperture Radar (SAR) images can provide detailed ground surface information. Thus, it is possible to observe a single building using HR SAR images. In this study, a new method is developed to detect building heights automatically from two-dimensional (2D) geographic information system (GIS) data and a single HR TerraSAR-X (TSX) intensity image. A building in a TSX image displays a layover from the actual position to the direction of the sensor, because of the side-looking nature of the SAR. Since the length of the layover on a ground-range SAR image is proportional to the building height, it can be used to estimate this height. We shift the building footprint obtained from 2D GIS data toward the sensor direction. The proposed method was applied to a TSX image of Lima, Peru in the HighSpot mode with a resolution of about 1 m. The results were compared with field survey photos and an optical satellite image, and a reasonable level of accuracy was achieved.

Keywords: TerraSAR-X, SAR intensity image, building height, building footprint, Lima

1. Introduction

Currently, more than half of the global human population lives in urban environments. Building inventory data are important for monitoring urban development and estimating its vulnerability. Although two-dimensional (2D) geographic information system (GIS) data, such as building footprints, have been generated for many urban areas from satellite or aerial images, height information is still insufficient.

In the last few years, imagery data from new high- resolution (HR) synthetic aperture radar (SAR) sensors, e.g., Cosmo-SkyMed and TerraSAR-X (TSX), have provided us with more detailed ground surface information. The features of an individual urban structure, especially its height, have now become available from these SAR images. Although there have been several methods for obtaining height information from HR optical images, these methods were limited by the weather and daylight conditions [1, 2]. Several methods related to height detection from HR SAR images have been proposed, and they are divided into three categories.

The first category is interferometric (InSAR) analysis. Bolter and Leberl [3] extracted buildings and their heights from multiple-view InSAR datasets. Thiel et al. [4] used two approaches to detect buildings of different sizes from multi-aspect HR InSAR datasets. Building features were extracted independently for each direction from the amplitude and phase information in the InSAR data. These methods, however, require at least two SAR images from different flight angles. The second category is based on a direct electromagnetic backscattering model. Franceschetti et al. [5] proposed a method to extract building height information based on a radiometric analysis of the double-bounce contribution. They tested this method on an airborne SAR sensor image [6], while Liu et al. [7] applied the method to a TSX image of Shanghai, China. This method requires prior knowledge of the material and surface roughness properties of the background, and it cannot be used in different areas. The third category is based on the geometric characteristics of layover and radar-shadow areas. Xu and Jin [8] proposed a method for the automatic reconstruction of building objects from multi-aspect very HR SAR data. Brunner and Lemoine [9] estimated building heights by matching simulated SAR images with a real image containing buildings of various heights. However, these methods are complicated and time consuming.

This work focuses on an earthquake and tsunami disaster mitigation program in Peru [10]. To assess the tsunami

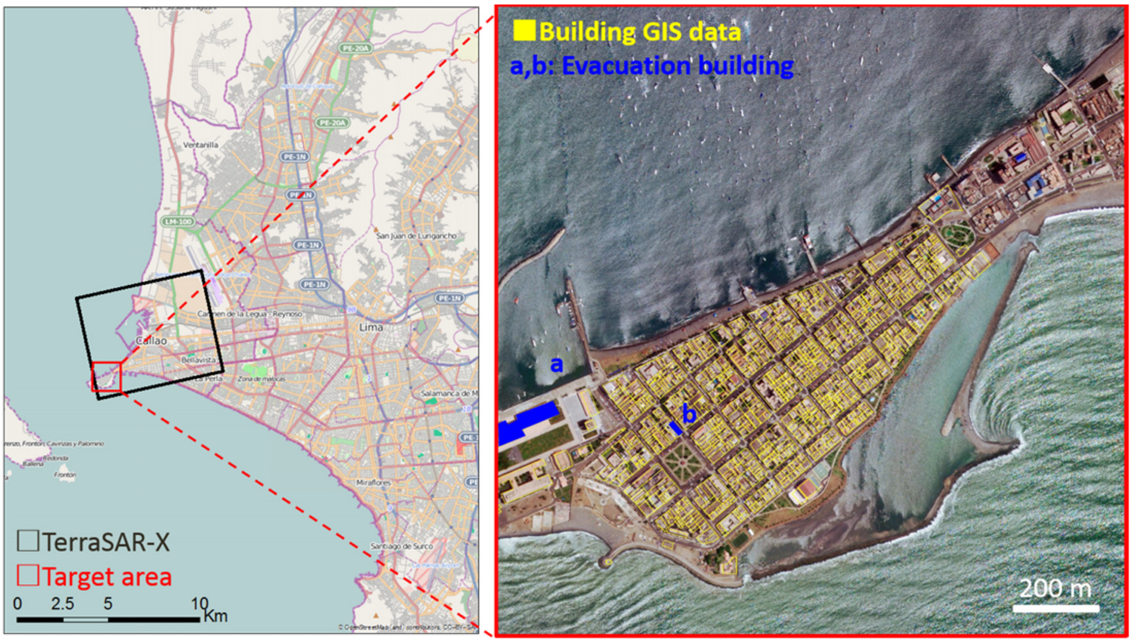

Fig. 1. Coverage of the TerraSAR-X image used in this study (black frame) and the WorldView-2 image taken on December 27, 2010 of the target area in the La Punta district (red frame) with the building block data and locations of two evacuation buildings.

(a) Escuela Naval (b) Jr. Saenz Pena cdra. 4

Fig. 2. Photos of a tsunami evacuation drill carried out on August 14, 2013. The participants gathered on the roofs of official evacuation buildings after the tsunami warning sirens. The locations of the two buildings are shown in **Fig. 1**.

risk in Lima, Peru, Mas et al. [11] simulated a tsunami inundation and human evacuation behavior. Adriano et al. [12] mapped a tsunami inundation area around the central zone of the Lima coast using two tsunami source scenarios. For tsunami simulations, detailed elevation data, e.g., building heights, is an important factor when evaluating the roughness coefficient of the surface. Thus, the 3D modeling of buildings is necessary to achieve this objective, and hence the use of HR SAR imagery is investigated here.

In this study, a simple method is proposed to detect the heights of individual buildings by estimating their layover lengths from a single HR SAR image. The proposed method belongs to the third type of approach, which has the fewest limitation and can be applied to various locations. The footprint of a single building taken from 2D GIS data is needed to create an initial template on a SAR image. The template is then shifted in the range direction of the sensor to distinguish the boundary of the layover. This method was applied to a TSX image of the La Punta district in the Lima metropolitan area of Peru. In addition, the visual interpretation of building heights from a WorldView-2 (WV-2) image was introduced as a reference to verify the accuracy of the proposed method.

2. Study Area and Image Data

2.1. La Punta District

The study focuses on a coastal area of the Lima metropolitan area, Peru, as shown in **Fig. 1**. The coastal plain rises about 15 m above sea level, however, the elevation of the La Punta district target area is less than 3 m. This district is surrounded by the Pacific Ocean on three sides and has been affected by several historical tsunamis. There are more than 5,000 residents living in La Punta, and hence tsunami inundation mapping and evacuation are important issues in disaster management.

As a part of the Science and Technology Research Partnership for Sustainable Development (SATREPS) Project, a tsunami evacuation drill was carried out in this district on August 14, 2013. Nineteen buildings were selected to be official evacuation buildings in La Punta. A vertical evacuation drill was conducted for the designated evacuation buildings. About 2,000 people participated in this drill. **Fig. 2** shows evacuees gathering on the roofs of two evacuation buildings, guided by evacuation officers after warning sirens were sounded. **Fig. 2(a)** is the Navy School ("Escuela Naval" in Spanish) building with a capacity of 3,000 people, and **Fig. 2(b)** is the four-storied building "Jr. Saenz Pena cdra. 4" with a capacity of 160 people. The flag hanging in front of the Navy School building indicates it is an evacuation building. The locations of these two buildings are shown in **Fig. 1**.

2.2. TerraSAR-X Image

TerraSAR-X is a radar earth observation satellite launched on June 15, 2007 by the German Aerospace Center (DLR) and EADS Astrium. It carried a SAR with a 31 mm wavelength (X-band) antenna. The resolution of the TSX sensor was up to 1 m in SpotLight mode, 3 m in StripMap mode, and 18 m in ScanSAR mode. The satellite flies in a sun-synchronous dusk-dawn orbit with an 11 day period. Because of its HR and radiometric accuracy, it is able to observe the details of a single building from TSX images. In addition, its twin satellite, TanDEM-X, was launched on June 21, 2010 to create a high accuracy worldwide digital elevation model (DEM).

A TSX image taken on February 18, 2008 was used in this study. The image was taken by the VV polarization in the ascending path. The image is taken in HighSpot (HS) mode, which is a HR SpotLight mode. The azimuth resolution is about 1.10 m and the ground range resolution is about 0.73 m. The incident angle is 53.9° at the center, and the heading angle is 347.6°. The image was recorded as a single-look slant-range complex (SSC) product.

2.3. Image Pre-Processing

Several pre-processing steps were carried out on the image prior to the detection of building heights. First, the TSX image was transformed into a geocoded ground range amplitude image using *ENVI/SARscape* software. To keep the high resolution, the number of looks for both the range and azimuth was set to one. A 5 m DEM for the target area was converted from topography data based on contour lines, as shown in **Fig. 3(a)**. The slant range TSX data was geocoded and calibrated by the obtained DEM. It was resampled at 0.5 m/pixel in a square size. According to the DLR specifications, the error of the achieved orbit accuracy is considered as below 20 cm [13]. Thus, the geocoded TSX image was considered to have high geo-accuracy. Next, after the radiometric calibration process, the image was transformed into a Sigma Naught (σ^0) value, which represents the radar reflectivity per unit area in the ground range. One of the most commonly used adaptive filters, the enhanced Lee filter [14], was used to reduce the speckle noise in the original SAR image that makes the radiometric and textural aspects less clear. To prevent the loss of the information included in the intensity images, the window size of the filter was set as small as possible, i.e., to 3×3 pixels (about 1.5×1.5 m). The TSX image after all the pre-processing steps is shown in **Fig. 3(b)**.

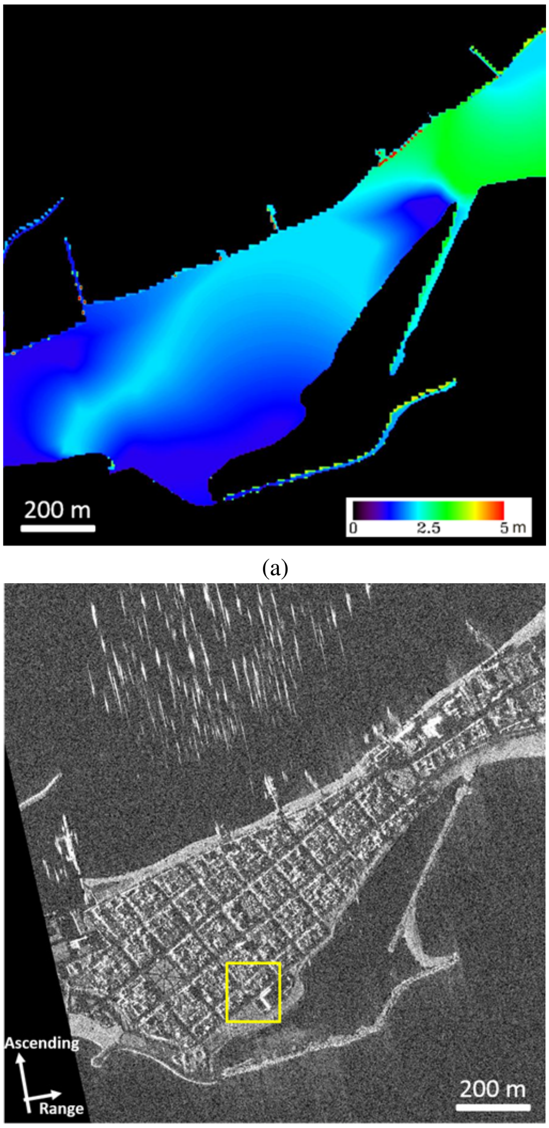

(a)

(b)

Fig. 3. DEM at 5 m resolution, converted from geometric data based on contour lines (a) and the pre-processed TerraSAR-X intensity image of the target area (b).

3. Methodology of Height Detection

Because of the side-looking nature of SAR, a building in a TSX image shows a layover from the actual position in the direction of the sensor, as shown in **Fig. 4**. The layover is proportional to the building height, as follows:

$$L = H/\tan\theta \qquad (1)$$

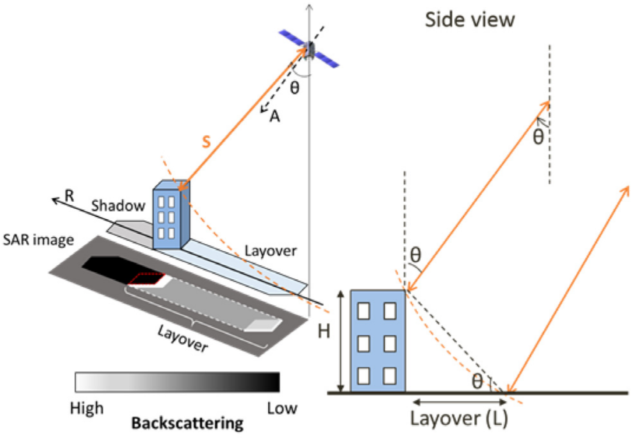

Fig. 4. Schematic plot of the location of a building in a SAR image.

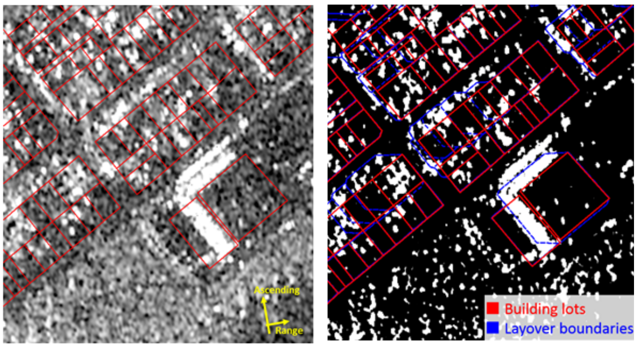

(a) (b)

Fig. 5. Close-ups of the TSX intensity image (a) and the converted binary image (b), with the building lot data (red) and the estimated boundaries of the layovers (blue).

where θ is the radar incident angle for the TSX image. Thus, the length of the layover can be used to measure the building height.

A close up of the TSX intensity image is shown in **Fig. 5(a)**. From only a single TSX image, it is difficult to distinguish the layover areas of buildings. Thus, outline data of buildings were introduced. Because there was no building footprint data available in Peru, a 2D GIS map including lot boundaries was instead used in this study. The outlines are indicated in **Fig. 1** by black lines, and a close-up is shown in **Fig. 5(a)**, overlaid on the TSX image. Although the number of stories for each building is included in the GIS data, more accurate building height information is useful for a tsunami evacuation analysis.

From **Fig. 5(a)**, it is obvious that high backscatter areas caused by building walls lie outside the building footprint. If the length of layover in the sensor direction is detected, the height of the building can be calculated using Eq. (1).

3.1. Generation of Layover Template

To detect layover length, a template was created based on the building outline and was then shifted in the direction of the SAR sensor (southwest). Since a normal building is usually higher than 2 m, this was the initial height for measuring a layover area. Because of the 53.91° incidence angle and 347.65° path angle (clockwise from the north), a 2-m building shows a 2.36-m layover to the west and a 0.41-m layover to the south. The width of the layover increases by 0.73 m to the west and 0.16 m to the south for every 1-m increase in building height.

Considering the resolution and pixel size of the TSX image, the width of the template was set for a 0.5-m building height. Thus, the initial template for the layover of a wall with a height between 2.0 and 2.5 m was created, as shown in the red block in **Fig. 6(a)**. Because most of the layovers occur on streets, the area within the building outline was removed from the template. Thus, the shape of the template depends on the size of the building and surrounding conditions.

In theory, a building of 5×5 m^2 would have a template of about 2.2 m^2. However, in the case of buildings arranged in row, the layover area is seen only in one direction and is relatively small. To confirm that there is enough information within a template, a single template should be larger than 1.0 m^2. If the initial template is not large enough, as when it is surrounded by other buildings, a layover measurement will not begin. The created template is shifted in the direction of the sensor, step by step, by increasing the building height at intervals of 0.1 m. To improve the accuracy of the height detection, the area in the TSX image surrounding a building was resampled to 0.1 m by cubic convolution (1/5 of the initial pixel size). When the template leaves the layover area, the final height is obtained.

3.2. Estimation of Layover Boundary

To estimate the boundary of the layover, two threshold methods were used. The first defines the threshold value with respect to the backscattering intensity. The average value of the backscatter in the TSX image within the template is calculated. When it is lower than the threshold value, the template is classified as a street and its shifting is stopped. However, this method shows errors when there is an outstanding bright or dark object within the template.

The second method uses a threshold defined with respect to areal percentage. In this method, the TSX image is first divided into a binary image using one threshold value. High backscatter areas such as corner reflections and the layover of walls are labeled “1,” whereas low backscatter areas such as radar shadows and roads are labeled “0.” Next, the percentage of high backscatter areas within a template is calculated. When the percentage is lower than a threshold value, the template is classified as a street. In this study, the latter method was selected. The TSX image was divided by the average backscattering intensity of the entire image, which is -10.5 dB. A portion of the binary image is shown in **Fig. 5(b)**.

Next, the threshold value for the areal percentage was investigated for 10 buildings as an example. The sample buildings are shown in **Fig. 7** by bold black lines. According to the GIS data, the maximum number of floors in a building in this area is nine. Thus, the maximum building

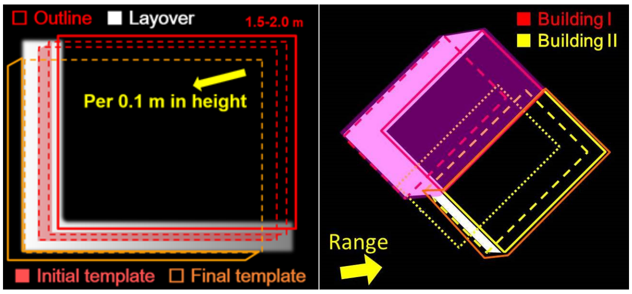

(a) (b)

Fig. 6. Simulation of the template for layover measurement (a) and boundary definition for two connected buildings with different heights (b).

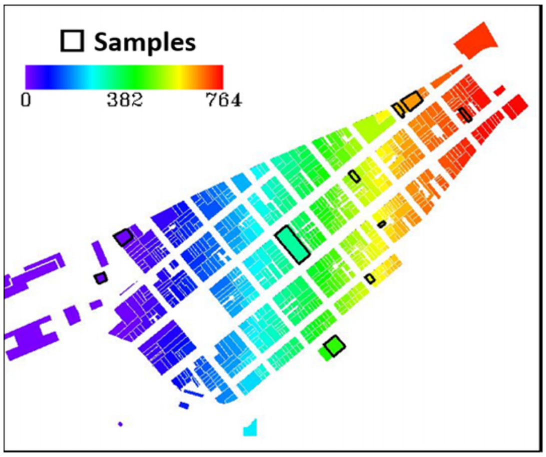

Fig. 7. ID numbers were assigned to 764 buildings according to their distance from the SAR sensor.

height was set to 30 m, meaning that the maximum distance for determining the width of a layover is 21.50 m to the west and 4.71 m to the south. The percentage value within a template for each building was recorded as shifting the template. To remove noise, a filter was applied to smooth the percentage values by averaging over 10 consecutive values. The smoothed percentage values were normalized by their maximum values, as shown in **Fig. 8**.

It was confirmed that the percentage value in a template is the highest at the beginning and reduces as the template is shifted. However, when the template is shifted over another building, the percentage value increases again. Thus, once the percentage value is lower than a threshold value, the last template location is used to estimate the height in this study. According to the number of building stories in the GIS data, a reference height was obtained by multiplying the number of stories by 3 m, which is regarded as the average height of one story. The percentage values for these samples given the reference heights were obtained and averaged to determine the final threshold value, which is 52%. Thus, once the smoothed standardized percentage value reaches less than 52%, the last location of the layover is considered to be the boundary. An example of the building with ID 534 is shown in **Fig. 8**. It is a one-story building, and its estimated height is 4.6 m (between one and two stories).

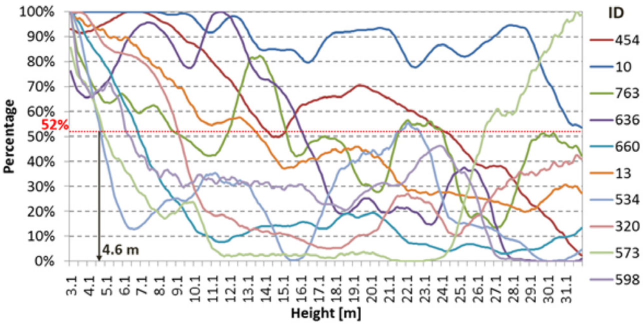

Fig. 8. Percentages for the sample buildings shown in **Fig. 7**, after smoothing by averaging over 10 consecutive values and normalized by their maximum; when the percentage is less than 52%, the final height is defined.

3.3. Building Orders

When there are two buildings of different heights with no space between them, their layover areas, which have different lengths, are also connected, as shown in **Fig. 6(b)**. If two building templates shift at the same time, the template for Building II, indicated by a yellow dotted line, will measure both layover areas. In this case, the height of Building II cannot be detected correctly. Thus, the order of the layover measurement is important. In this study, to confirm that template shifting was performed in the correct order, an ID number was assigned to each building. A smaller ID number was assigned to buildings located closer to the direction of sensor. Next, the templates were created and shifted in the order of ascending ID number. Once a layover area has been measured, it was masked and not measured again. As seen in the case of **Fig. 6(b)**, the layover area of Building I was measured first and the final boundary is indicated by a red dashed line. Next, the area of Building I and its layover area were masked when measuring the layover of Building II. Finally, the boundary of Building II was detected correctly; this boundary is indicated by a yellow dashed line.

4. Detected Results and Verification

The proposed method was applied to the target area shown in **Fig. 3**. According to the GIS data, 764 buildings exist there. They were numbered based on their distances from the SAR sensor, as shown in **Fig. 7**. The layover areas were measured in the order of their ID numbers, and their lengths were used to calculate the building heights. The maximum height of the layover measurement was 30 m, equal to the height of a ten-story building. The heights of 398 buildings were detected successfully, and the results are shown in **Fig. 9(a)**. Some buildings could not be detected because of their surrounding conditions. Most of these buildings were located behind other buildings, where there was no space to create a template.

A reference height was obtained from the number of stories in the GIS data, as shown in **Fig. 9(b)**. Comparing **Figs. 9(a)** and **(b)**, we observe that several buildings are

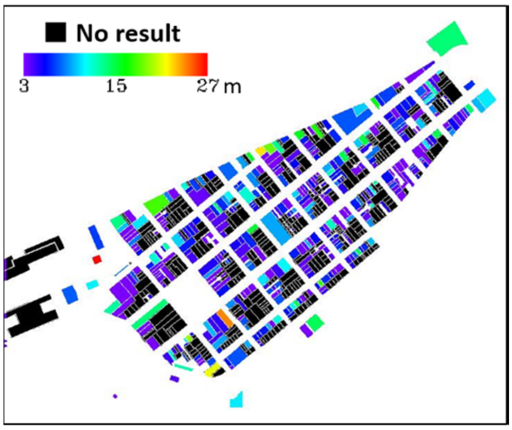

(a) Estimated height

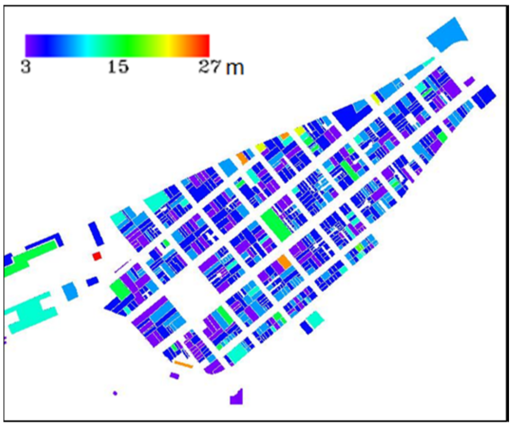

(b) GIS height

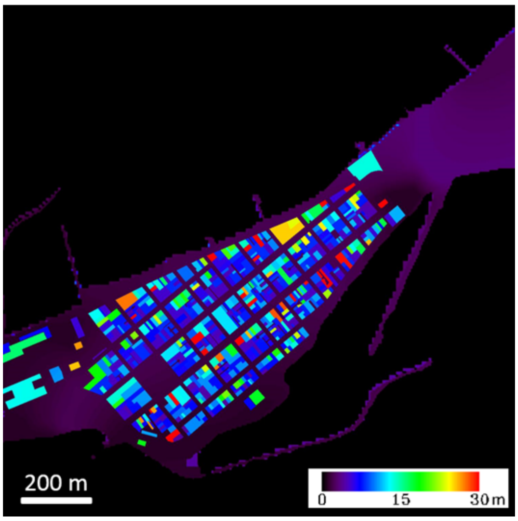

(c) DSM

Fig. 9. Heights for 398 buildings calculated by the proposed method (a), reference building heights obtained by multiplying the number of stories by 3 m (b), and the final DSM by combining the estimated results and GIS heights (c).

shown in a similar color, indicating that they have similar heights. Because the real heights of the buildings are unknown, it is difficult to verify the accuracy of the proposed method. Thus, two methods were used in this study to verify the estimated results. The first was a comparison with the GIS data, and the second was a visual interpretation of an HR optical image from the WV-2 satellite.

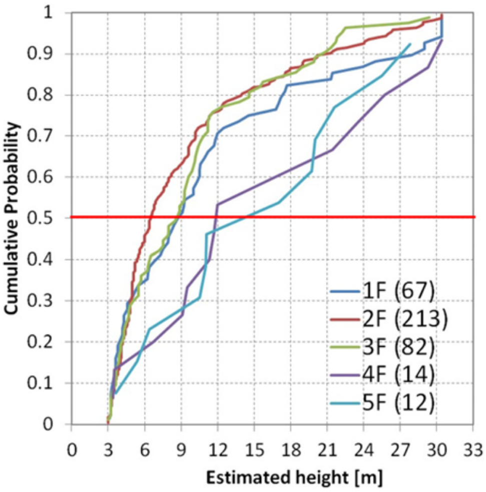

Fig. 10. Detected heights grouped by number of stories (F) from the GIS data on a cumulative distribution plot.

Table 1. Number of estimated buildings and their median heights for each number of stories.

Number of stories	1	2	3	4	5
Number of buildings	67	213	82	14	12
Median height [m]	8.7	6.5	8.7	12.0	17.0

In addition, a digital surface model (DSM) was built by combining the DEM, estimated building heights, and heights converted from the GIS data, as shown in **Fig. 9(c)**. For the 398 buildings that could be estimated by our method, the results were added to the original elevation. For the remaining buildings, the heights, converted from the number of stories, were used. This DSM could help improve the accuracy of tsunami inundation mapping and evacuation simulations.

4.1. Comparison with GIS Data

The estimated height was compared with the number of stories in the GIS data. The results were grouped by the number of stories in each building. The heights in each group were then sorted in ascending order. The cumulative probability of the estimated height for each building with respect to number of stories was calculated, as shown in **Fig. 10**. The height with a probability of 0.5 is the median height for this group. Considering the number of buildings in each group, the cumulative distributions were drawn for one- to five-storied buildings only.

From **Fig. 10**, it can be confirmed that the median values of the estimated heights increase as the number of stories increases. However, the median height for one-storied buildings was 8.7 m, which equals the average height for three-storied buildings. The median heights for one- to five-storied buildings are shown in **Table 1**. Except for the one-storied buildings, the median values of the estimated heights were similar to the values obtained by multiplying the number of stories by 3 m.

The errors for one-storied buildings were caused in the layover measurement step. Because the layover measurement starts at 2.5 m, the layover area for a one-storied building is very small. After the smoothing and standardizing process for recording percentage values from 2.5 to 30.0 m, the value of the layover becomes smaller than the actual value. Therefore, it is difficult to distinguish the layover of one-storied buildings from street areas. However, the proposed method can estimate the height of individual buildings two stories or taller. Another basic reason for the errors is the building footprint data. Since the outline of each lot was used as a building footprint in this study, the differences among them caused errors in the layover measurement step. The accuracy of our proposed method would be improved by introducing more accurate footprint data.

4.2. Comparison with the WorldView-2 Image

A WV-2 image, taken on December 27, 2010 and shown in **Fig. 1,** was used to verify the accuracy of the proposed method, as shown in **Fig. 11(a)**. The ground resolution for this panchromatic image is 0.50 m, which is the same as the pixel size of the pre-processed TSX image. According to [1, 15], the height of an individual building can be estimated from an HR optical satellite image by

$$H = \frac{D}{\sqrt{\dfrac{1}{\tan^2\lambda'} + \dfrac{1}{\tan^2\lambda} - \dfrac{2\cos(\alpha-\alpha')}{\tan\lambda'\cdot\tan\lambda}}} \quad . \; . \quad (2)$$

where D is the distance between the top point of the building and the same point on its shadow in the satellite image; the azimuth and elevation angles of the satellite are α and λ, respectively; and the azimuth and elevation angles of the sun are α' and λ', respectively.

Ten buildings were selected (excluding the samples used to define the threshold value), as indicated in **Fig. 11(a)** by cyan lines. The lengths L for these buildings were manually measured from the WV-2 image to estimate their heights. An example is shown in **Fig. 11(b)**. According to the header file of the WV-2 image, the azimuth angle of the sun is 103.3° and its elevation angle is 65.2°. The azimuth angle for the satellite is 255.7° while the elevation angle is 72.6°. Because the measured distance of D in **Fig. 11(b)** is 20 pixels, the height of this building was measured to be about 13.3 m by Eq. (2). The height estimated from the TSX image by our method is 17.7 m. The heights for ten buildings were obtained, as shown in **Table 2**. A comparison of the detected and reference heights is shown in **Fig. 12**.

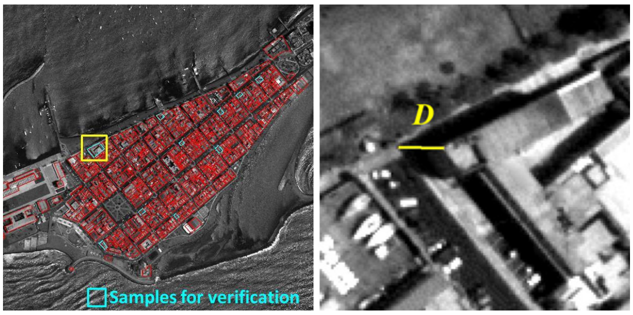

(a) (b)

Fig. 11. Detected heights for 398 buildings by the proposed method (a), and reference building heights obtained by multiplying the number of stories by 3 m (b).

Table 2. Estimated heights from the TSX image compared to heights from the WorldView-2 image measured by visual interpretation. Unit: m

ID number	TSX	WV-2	Difference
51	7.30	7.4	0.10
87	7.30	5.2	-2.10
226	8.62	5.9	-2.72
304	9.95	9.9	-0.05
381	6.96	4.4	-2.56
406	13.93	17.7	3.77
585	11.27	10.1	-1.17
592	5.97	6.1	0.13
667	10.61	8.6	-2.01
709	21.89	22.1	0.21

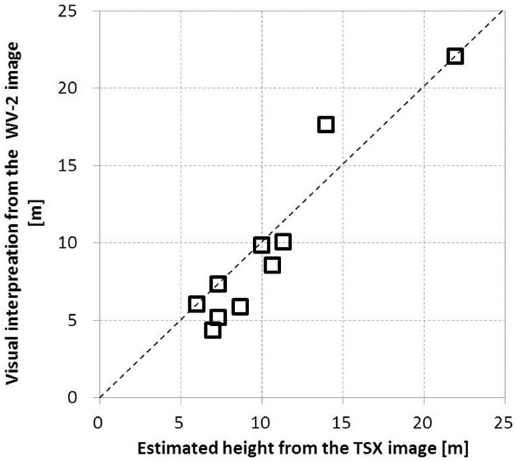

(b)

Fig. 12. Estimated building heights compared to the visual interpretation results from the WV-2 image.

From the figure, it could be confirmed that the estimated heights from the TSX image are very close to the result of visual interpretation from the WV-2 image. The maximum difference between the estimated height by the layover method and the result from visual interpretation was 3.77 m. Most of the differences were less than 3 m, the average height of one story. The average value of the differences is −0.64 m, while the Root Mean Square (RMS) error is 1.95 m, also less than the average height of one story.

Because the corresponding highest points for both the building and its shadow are needed, the heights of many buildings could not be measured by visual interpretation. In addition, visual interpretation requires time and effort. On the contrary, our proposed method can estimate building heights automatically from a single TSX image, and its result is similar to that of visual interpretation. Thus, it is more efficient than visual interpretation using HR optical images.

5. Conclusions

In this study, a method to detect the height of an individual building from an HR TerraSAR-X (TSX) image was proposed by measuring the length of layovers. The method was tested using a 1-m resolution SAR image of La Punta, in the Lima metropolitan area of Peru. The outlines of 764 building lots from GIS data were overlaid on the TSX image to detect the building heights. As a result, the heights of 398 buildings were detected successfully. The estimated building heights were compared with the number of stories recorded in the GIS data and a visual interpretation result from a WV-2 optical satellite image. By plotting the cumulative distribution of the estimated heights of buildings, the median height for buildings was similar to three times the story number. Because the normal average height for one story is about 3 m, our method estimates the building height accurately.

Ten buildings were selected as samples to verify the accuracy of the estimated results. Their heights were manually measured from the WV-2 image. Comparing the estimated results from the TSX image with those from the visual interpretation, the average difference for ten samples was -0.64 m and the RMS error was 1.95 m, less than the height of a single story.

There still exist some errors in the estimated results. The accuracy of the proposed method depends on the surrounding conditions of the target building and the shape of its footprint. Because the outlines of lots were used instead of those of the buildings, many mismatches occurred in the layover measurement step. However, the results show that our method is generally useful for estimating building height. Finally, a detail DSM was built by combining the original DEM, estimated results, and GIS data.

In the future, this method will be tested on more HR SAR images of different locations to verify its accuracy and examine its limitations. Our method is a convenient way to create a 3D city model for tsunami inundation and human evacuation simulations.

Acknowledgements

TerraSAR-X data is the property of DLR and the Inforterra GmbH. This study was supported in part by the Japan Science and Technology Agency (JST) and Japan International Cooperation Agency (JICA) within the SATREPS framework, "Enhancement of Earthquake and Tsunami Disaster Mitigation Technology in Peru."

References:

[1] X. Huang and L. K. Kwoh, "3D building reconstruction and visualization for single high resolution satellite image," Proc. IEEE IGARSS 2007, pp. 5009-5012, 2007.

[2] X. Hou, M. Qi, D. Li, G. Lv, and Y. Wang, "2011. The model of extracting the height of buildings by shadow in image," Pro. ICCSNT 4, pp. 2150-2153, 2011.

[3] R. Bolter and F. Leberl, "Detection and reconstruction of human scale features from high resolution interferometric SAR data," Pro. 15th Int. Conf. Pattern Recognition, Vol.4, pp. 291-294, 2000.

[4] A. Thiel, E. Cadario, K. Schulz, U. Thoennessen, and U. Soergel, "Building recognition from multi-aspect high-resolution InSAR data in urban areas," IEEE Trans. Geoscience and Remote Sensing, Vol.45, No.11, pp. 495-505, 2007.

[5] G. Franceschetti, A. Iodice, and D. Riccio, "A canonical problem in electromagnetic backscattering from buildings," IEEE Trans. Geoscience and Remote Sensing, Vol.40, No.8, pp. 1787-1801, 2002.

[6] G. Franceschetti, R. Guida, A. Iodice, D. Riccio, and G. Ruello, "Building feature extraction via a deterministic approach: Application to real high resolution SAR images," Proc. IEEE IGARSS 2007, pp. 2681-2684, 2007.

[7] K. Liu, T. Balz, and M. Liao, "Building height determination by TerraSAR-X backscatter analysis in dense urban areas," Proc. 2009 Asian Conference on Remote Sensing, 2009.

[8] F. Xu and Y.-Q. Jin, "Deorientation theory of polarimetric scattering targets and application to terrain surface classification," IEEE Trans. Geoscience and Remote Sensing, Vol.43, No.10, pp. 2351-2364, 2005.

[9] D. Brunner and G. Lemoine, "Building height retrieval from VHR SAR imagery based on an iterative simulation and matching technique," IEEE Trans. Geoscience and Remote Sensing, Vol.48, No.3, pp. 1487-1504, 2010.

[10] F. Yamazaki and C. Zavala, "SATREPS Project on Enhancement of Earthquake and Tsunami Disaster Mitigation Technology in Peru," Journal of Disaster Research, Vol.8, No.2, pp. 224-234, 2013.

[11] E. Mas, B. Adriano, and S. Koshimura, "An integrated simulation of tsunami hazard and human evacuation in La Punta, Peru," Journal of Disaster Research, Vol.8, No.2, pp. 285-295, 2013.

[12] B. Adriano, E. Mas, S. Koshimura, Y. Fujii, S. Yauri, C. Jimenez, and H. Yanagisawa, "Tsunami Inundation Mapping in Lima, for Two Tsunami Source Scenarios," Journal of Disaster Research, Vol.8, No.2, pp. 274-284, 2013.

[13] T. Fritz and M. Eineder, "TerraSAR-X Ground Segment Basic Product Specification Document," Issue 1.9, pp. 36-38, 2013, Available: https://www.google.co.jp/url?sa=t&rct=j&q=&esrc=s&source=web&cd=1&cad=rja&uact=8&ved=0CB0QFjAA&url=https%3A%2F%2Ftandemx-science.dlr.de%2Fpdfs%2FTX-GS-DD-3302_Basic-Products-Specification-Document_V1.9.pdf&ei=zYZgVOf3GOHWmAW4n4DIAw&usg=AFQjCNFYBxmuXJUDQqnFnEZqBp-B7l5FXw&sig2=8tCqa641FRq2KP4GUQV5fw&bvm=bv.79189006,d.dGY [accessed Nov. 10, 2014]

[14] A. Lopes, R. Touzi, and E. Nezry, "Adaptive Speckle Filters and Scene Heterogeneity," IEEE Trans. Geoscience and Remote Sensing, Vol.28, No.6, pp. 992-1000, 1990.

[15] Y. Iwasaki and F. Yamazaki, "Detection of building collapse from the shadow lengths in optical satellite images," Proc. 32nd Asian Conference on Remote Sensing, Taipei, Paper No.202, CD-ROM, p. 6, 2011.

Name:
Wen Liu

Affiliation:
Assistant Professor, Graduate School of Engineering, Chiba University

Address:
1-33 Yayoi-cho, Inage-ku, Chiba 263-8522, Japan

Brief Career:
2010-2013 Ph. D. of Engineering, Chiba University
2013-2014 JSPS Postdoctoral Fellowship for Foreign Researchers, Tokyo Institute of Technology
2014- Assistant Professor, Graduate School of Engineering, Chiba University

Selected Publications:

- "Extraction of Tsunami Flooded Areas and Damaged Buildings in the 2011 Tohoku, Japan Earthquake from TerraSAR-X Intensity Images," Earthquake Spectra, ERRI, Vol.29, No.S1, pp. S183-2000, March, 2013.

Academic Societies & Scientific Organizations:

- Japan Society of Civil Engineers (JSCE)
- Remote Sensing Society of Japan (RSSJ)
- Institute of Electrical and Electronics Engineers (IEEE)